

Article

Particle Production in Xe+Xe Collisions at the LHC within the Integrated Hydrokinetic Model

Yuri Sinyukov ^{1,2,*}, Musfer Adzhymambetov ¹ and Volodymyr Shapoval ¹

¹ Department of High-Density Energy Physics, Bogolyubov Institute for Theoretical Physics, 03143 Kiev, Ukraine; adzhymambetov@gmail.com (M.A.); shapoval@bitp.kiev.ua (V.S.)

² Department of Physics, Tomsk State University, Lenin Ave. 36, Tomsk 634050, Russia

* Correspondence: sinyukov@bitp.kiev.ua

Received: 15 December 2019; Accepted: 5 February 2020; Published: 18 February 2020



Abstract: The paper is devoted to the theoretical study of particle production in the Large Hadron Collider (LHC) Xe+Xe collisions at the energy $\sqrt{s_{NN}} = 5.44$ TeV. The description of common bulk observables, such as mean charged particle multiplicity, particle number ratios, and p_T spectra, is obtained within the integrated hydrokinetic model, and the simulation results are compared to the corresponding experimental points. The comparison shows that the model is able to adequately describe the measured data for the considered collision type, similarly as for the cases of Pb+Pb LHC collisions and top Relativistic Heavy Ion Collider (RHIC) energy Au+Au collisions, analyzed in our previous works.

Keywords: xenon; heavy-ion collision; LHC; particle momentum spectrum; particle number ratio

1. Introduction

The study of particle production in relativistic heavy-ion collisions is important for understanding the dynamics of the evolution of hot and dense systems formed in these processes. The investigation of such complicated phenomena is much more effective when the analysis of the experimental data is accompanied by simulations within a realistic model of the collision. Theoretical analysis often allows finding the most adequate interpretation of the measured data, clarifying the role of specific factors in the formation of observed results, and understanding the interplay (often quite complicated) between these factors.

In the recent papers [1–3], the integrated hydrokinetic model (iHKM) [4] was applied to the description of particle production in Au+Au collisions at the top RHIC energy $\sqrt{s_{NN}} = 200$ GeV and Pb+Pb collisions at the LHC energies $\sqrt{s_{NN}} = 2.76$ TeV and $\sqrt{s_{NN}} = 5.02$ TeV. The analysis of the particle momentum spectra, particle yields, and particle number ratios shows in particular that a successful description of the data can be reached in the model even using different equations of state for quark-gluon matter at the hydrodynamics stage of expansion, if the initial energy-density profile is correspondingly rescaled. The particle number ratios, calculated with inelastic processes switched off at the final “afterburner” stage of the collision, differ from the same ratios calculated in “full mode” (i.e., when the inelastic processes are taken into account) and, unlike the latter, depend on the utilized equation of state. This fact shows the importance of the afterburner particle scatterings for the formation of the observed ratio values.

In the article [5], a conclusion about great influence of intensive particle interactions with the hadronic medium at the late stage of the collision on the number of detected $K^*(892)$ resonances (which were reconstructed in the experiment through the products of their decay $K^*(892) \rightarrow K\pi$) was made based on the results of iHKM simulations. The numerous hadronic interactions, leading to multiple rescatterings and recombinations of resonance decay products, also resulted in larger

estimated times of maximal emission (Since in iHKM, we do not have a sudden kinetic freeze-out, but particles emit continuously from the system, we utilize the time of maximal emission $\tau_{m.e.}$ concept in our studies. For particles of a certain species and from a certain p_T bin, $\tau_{m.e.}$ defines a spacelike hypersurface $\tau = \tau_{m.e.}$ with a thin 4D layer, adjacent to it, from which most of considered particles are emitted.) for kaons as compared to pions, as showed the analysis of the particle emission pictures, obtained from iHKM in the considered cases [1,6].

The mentioned results suggest that chemical and kinetic “freeze-out” in relativistic A+A collisions is rather continuous, not sudden. Such a conclusion looks reasonable, since sudden chemical freeze-out would mean an abrupt switching from the expansion of chemically equilibrated matter with very intensive inelastic reactions to the evolution of the system, where inelastic reactions are absent. As for a sudden kinetic freeze-out, it would suppose a sudden switching from very large hadron-hadron interaction cross-sections (in a nearly perfect hydrodynamics regime) to zero cross-sections (specific for the free streaming particles case). Both sharp transitions can hardly be expected from the theoretical point of view.

In the present work, we aim to apply iHKM to the description of particle production in Xe+Xe collisions at the LHC energy $\sqrt{s_{NN}} = 5.44$ TeV and find out if the results will be similar to those obtained in our previous studies.

2. Results and Discussion

In order to simulate the process of matter evolution during a high-energy heavy-ion collision, we utilized the integrated hydrokinetic model [2,4]. It consists of several blocks, each modeling a certain stage of collision. The first block deals with the early prethermal system’s dynamics, in the course of which it gradually transforms from the initial, non-thermalized state to the state of local equilibrium (chemical and thermal). To describe this process in iHKM, we simulated the evolution of the energy-momentum tensor of the system within an energy-momentum transport approach in a relaxation time approximation.

To obtain the initial conditions (i.e., the initial non-thermal energy-momentum tensor) for the pre-equilibrium stage, we used a combined approach: our tensor $T^{\mu\nu}(x)$ is defined by the initial distribution function $f(x, p)$, so that $T^{\mu\nu}(x) = \int d^3p f(x, p) p^\mu p^\nu / p^0$. The $f(x, p)$ can be factorized into space-time and momentum parts. The form of the momentum part of the function is based on the color glass condensate approach:

$$f_0(p) = g \exp \left(- \sqrt{ \frac{(p \cdot U)^2 - (p \cdot V)^2}{\lambda_\perp^2} + \frac{(p \cdot V)^2}{\lambda_\parallel^2} } \right), \quad (1)$$

where $U^\mu = (\cosh \eta, 0, 0, \sinh \eta)$, $V^\mu = (\sinh \eta, 0, 0, \cosh \eta)$, η is space-time rapidity, and initial momentum anisotropy $\Lambda = \lambda_\perp / \lambda_\parallel = 100$ [4]. The spatial part of the initial distribution function is generated by the GLISSANDOcode [7], which implements the Monte Carlo Glauber model. It gives us the initial transverse energy-density profiles $\epsilon(b, \mathbf{r}_T)$ (here, \mathbf{r}_T is the transverse plane radius vector and b is the impact parameter, denoting the collision centrality class):

$$\epsilon(b, \mathbf{r}_T) = \epsilon_0(\tau_0) \frac{(1 - \alpha)N_w(b, \mathbf{r}_T)/2 + \alpha N_{bin}(b, \mathbf{r}_T)}{(1 - \alpha)N_w(b = 0, \mathbf{r}_T = 0)/2 + \alpha N_{bin}(b = 0, \mathbf{r}_T = 0)}. \quad (2)$$

The coefficient $\epsilon_0(\tau_0)$ here is the main iHKM parameter, which allows adjusting the model to the description of different types of collisions, the initial energy density in the center of the system at the initial proper time being τ_0 . The other parameter α defines the proportion between the contributions $N_{bin}(b, \mathbf{r}_T)$ and $N_w(b, \mathbf{r}_T)$ from the “binary collisions” and the “wounded nucleons” models to the GLISSANDO energy-density profile. Note, that the quadrupole deformation of somewhat prolate xenon nuclei with deformation parameter $\beta_2 = (0.18 \pm 0.02)$ [8] also can be taken into account within the GLISSANDO code (for this purpose, the spherical nuclear radius R_0 is substituted in simulations

by the polar angle θ -dependent value $R(\theta) = R_0[1 + \beta_2 Y_2^0(\theta) + \beta_4 Y_4^0(\theta)]$, where Y_2^0, Y_4^0 are spherical harmonics. For the current study, we used the GLISSANDO profiles, generated with $\beta_2 = 0.18$.

After the prethermal stage follows the second iHKM block, which describes the hydrodynamical expansion of locally thermalized matter, using the relativistic viscous hydrodynamics approach based on the Israel–Stewart formalism. The energy-momentum tensor $T^{\mu\nu}(x)$ of the system now acquires the hydrodynamical form and gives us the hydrodynamical values of local energy density $\epsilon(x)$, pressure $p(x)$, and collective velocity $u^\mu(x)$. The shear viscosity to entropy ratio η/S is assumed to equal its minimal theoretical value $1/(4\pi) \approx 0.08$, which was calibrated in [2] as giving the best description of experimental data for Pb+Pb LHC collisions at 2.76A TeV.

The third stage in iHKM describes the particlization of the system, when we switch from describing it in terms of a continuous medium to the description in terms of particles. We assumed that the particlization took place at the isotherm hypersurface with temperature T_p , which in the general case depends on the used equation of state (EoS) for quark-gluon matter. The latter is matched at $T = T_p$ with the EoS of an ideal chemically equilibrated hadron-resonance gas, consisting of $N = 329$ well-established hadron states.

The switching hypersurface σ_{sw} is constructed in the course of the hydrodynamic evolution of the system using the Cornelius code [9–11]. The Cooper–Frye prescription is applied to convert the fluid to particles:

$$p^0 \left. \frac{d^3 N_i(x)}{d^3 p} \right|_{d\sigma(x)} = d\sigma_\mu(x) p^\mu f_i(p \cdot u(x), T(x), \mu_i(x)), \quad (3)$$

where $d\sigma(x)$ is the particlization hypersurface element near point x and i enumerates the particle species. The Grad ansatz is utilized to account for the viscous corrections to the equilibrium distribution function $f_i^{eq}(x, p)$ [12]. The corrections are assumed to be the same for all hadron species. Thus, the Equation (3) can be rewritten (in the fluid local rest frame) as:

$$\frac{d^3 \Delta N_i}{dp^* d(\cos\theta) d\phi} = \frac{\Delta\sigma_\mu^* p^{*\mu}}{p^{*0}} p^{*2} f_i^{eq}(p^{*0}; T, \mu_i) \left[1 + (1 \mp f_i^{eq}) \frac{p_\mu^* p_\nu^* \pi^{*\mu\nu}}{2T^2(\epsilon + p)} \right], \quad (4)$$

where $\pi^{*\mu\nu}$ is the shear stress tensor.

The particle coordinates and momenta are generated according to distributions (4) using the Monte Carlo procedure, so that the total hadron multiplicity in each event is randomly sampled in accordance with the Poisson distribution with a mean value equal to the mean total number of particles N_{tot} at the switching hypersurface σ_{sw} , which is calculated based on (4). The sort for each generated particle is chosen randomly with probability N_i/N_{tot} , where N_i is the mean number of hadrons of sort i at σ_{sw} according to (4).

At the next, final stage of the evolution, the generated particles, which now form our system, undergo multiple elastic and inelastic scatterings, and all possible resonance decays take place. This final block in iHKM was realized with the help of the UrQMDmodel [13,14].

As compared to other collision models utilizing the hybrid (hydro+cascade) approach (see, e.g., [15–19]), which succeed in reproducing the experimental data on soft observables in high-energy heavy-ion collisions, iHKM has an important advantage: the first prethermal stage of the matter evolution in iHKM allows one to describe the development of collective flow and other effects adequately, which starts due to the finiteness and azimuthal asymmetry of the system already at the early initial time $\tau_0 \approx 0.1$ fm/c, when the matter is not yet thermalized. This allows iHKM to describe all main bulk observables together with the femtoscopy radii for different collision types simultaneously.

The model parameter values that allow describing Xe+Xe collisions at 5.44A TeV were fixed as those giving the best agreement with the experimental mean charged particle multiplicity dependency on centrality (see Figure 1) and the pion spectrum for the most central events. The $\epsilon_0 = 445$ GeV/fm³ at $\tau_0 = 0.1$ fm/c and $\alpha = 0.44$ values were obtained from these fits. The chosen maximal energy density

value ϵ_0 was between that for the top RHIC energy Au+Au collisions ($235 \text{ GeV}/\text{fm}^3$) and the one for $2.76A \text{ TeV}$ Pb+Pb LHC collisions ($679 \text{ GeV}/\text{fm}^3$). The Xe+Xe value of α was the maximal among those used in our studies so far (for top RHIC energy case $\alpha = 0.18$ and for both Pb+Pb LHC cases $\alpha = 0.24$). A relatively large α value for Xe+Xe collisions as compared to the Pb+Pb collisions with close energy, which corresponds to a larger binary collision contribution to the initial energy-density distribution, can be connected with a smaller size of the Xe nucleus in comparison with the Pb nucleus. For quark-gluon phase at the hydrodynamics stage, the HotQCD Collaboration's equation of state was applied in current analysis [20] with particlization temperature $T_p = 156 \text{ MeV}$.

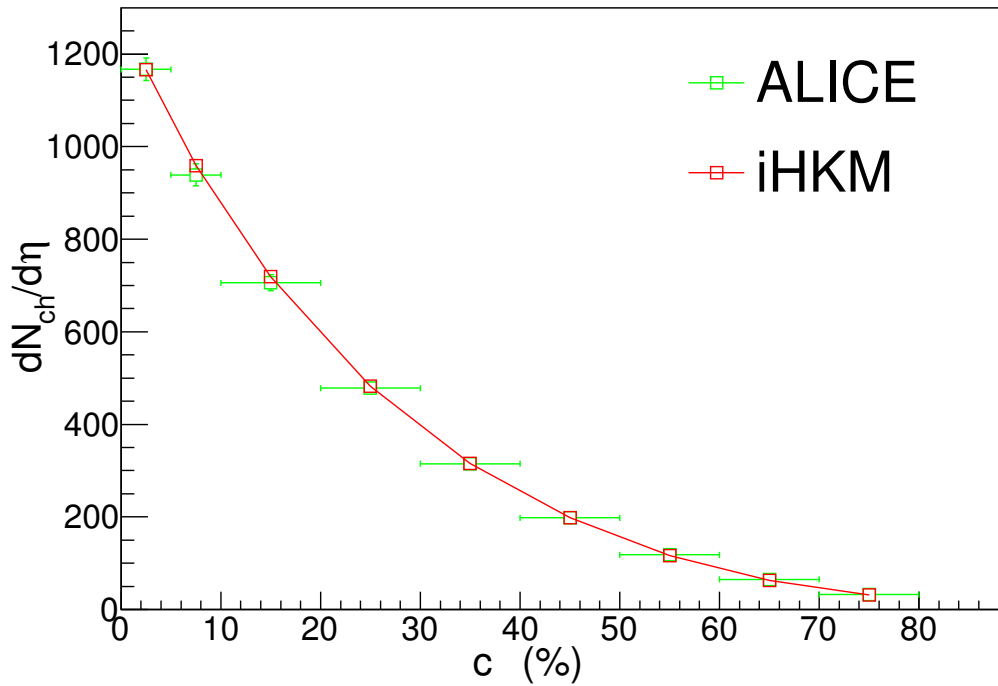


Figure 1. The mean charged particle multiplicity $\langle dN_{ch}/d\eta \rangle$ for $|\eta| < 0.5$ in Xe+Xe collisions at the LHC energy $\sqrt{s_{NN}} = 5.44 \text{ TeV}$ for different centrality classes calculated in the integrated hydrokinetic model (iHKM) and measured by the ALICE Collaboration [8].

In Figures 2–5, the transverse momentum spectra for all charged particles, pions, kaons, and protons calculated in the integrated hydrokinetic model for eight centrality classes are demonstrated together with the corresponding experimental data from the ALICE Collaboration [8,21]. From the plots, one can see that the model describes the experimental p_T spectra for all the particle species and all the centrality classes quite well. Note in particular that iHKM reproduces the measured pion spectra in a wide p_T interval, including the region of soft momenta. A similar description quality was reached earlier in [3,4] for $2.76A \text{ TeV}$ and $5.02A \text{ TeV}$ Pb+Pb collisions at the LHC.

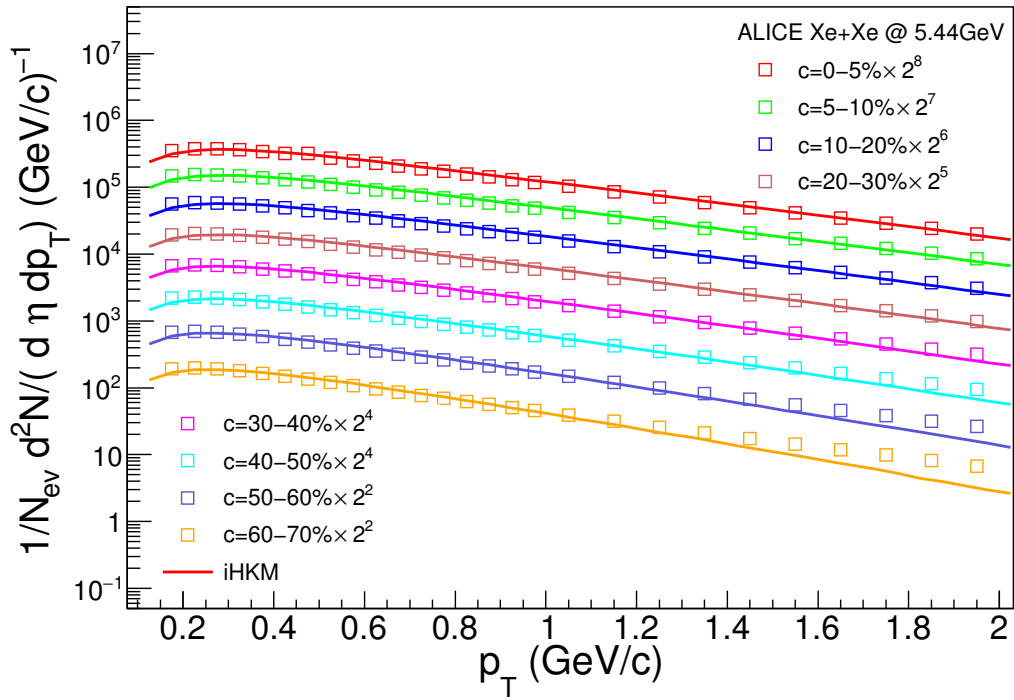


Figure 2. The iHKM results on transverse momentum spectra of all charged particles compared to the experimental data from the ALICE Collaboration [8] for Xe+Xe collisions at the LHC energy $\sqrt{s_{NN}} = 5.44$ TeV. The datasets for different centralities are scaled for better visibility, $|\eta| < 0.8$.

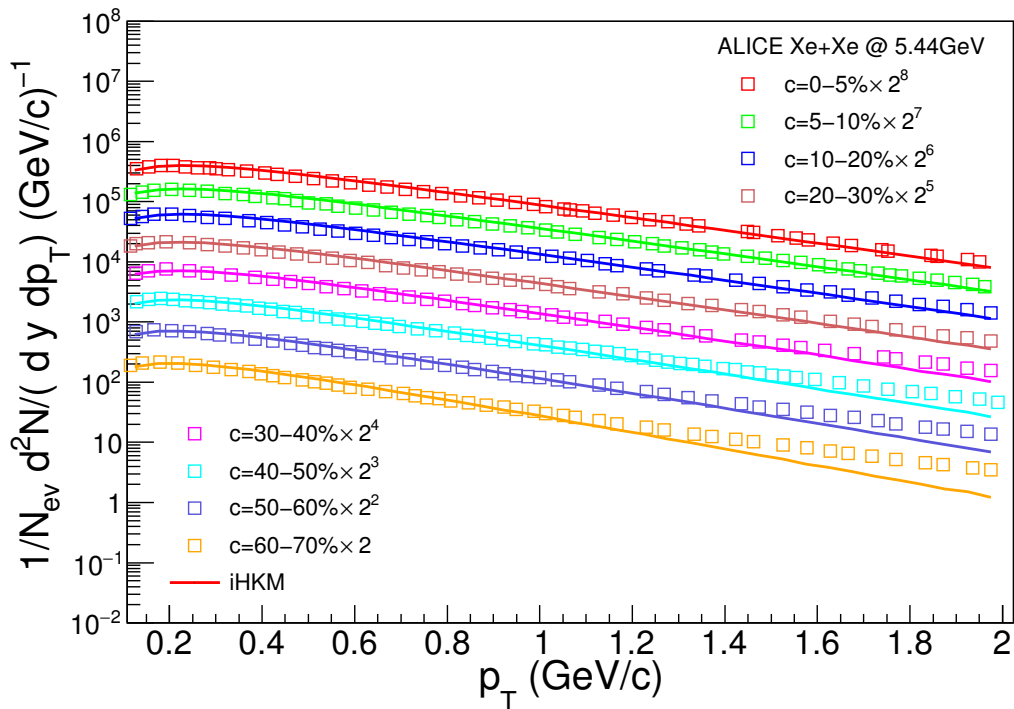


Figure 3. The same as in Figure 2 for pions, $|y| < 0.5$ (ALICE Collaboration points are taken from [21]).

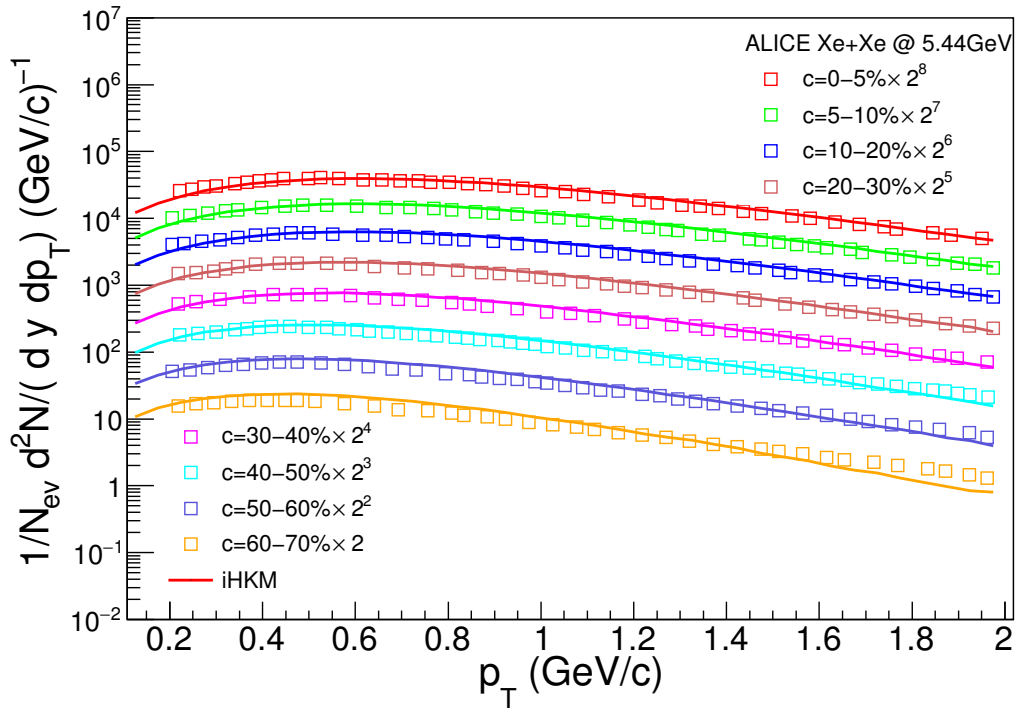


Figure 4. The same as in Figure 2 for kaons, $|y| < 0.5$ (ALICE Collaboration points are taken from [21]).

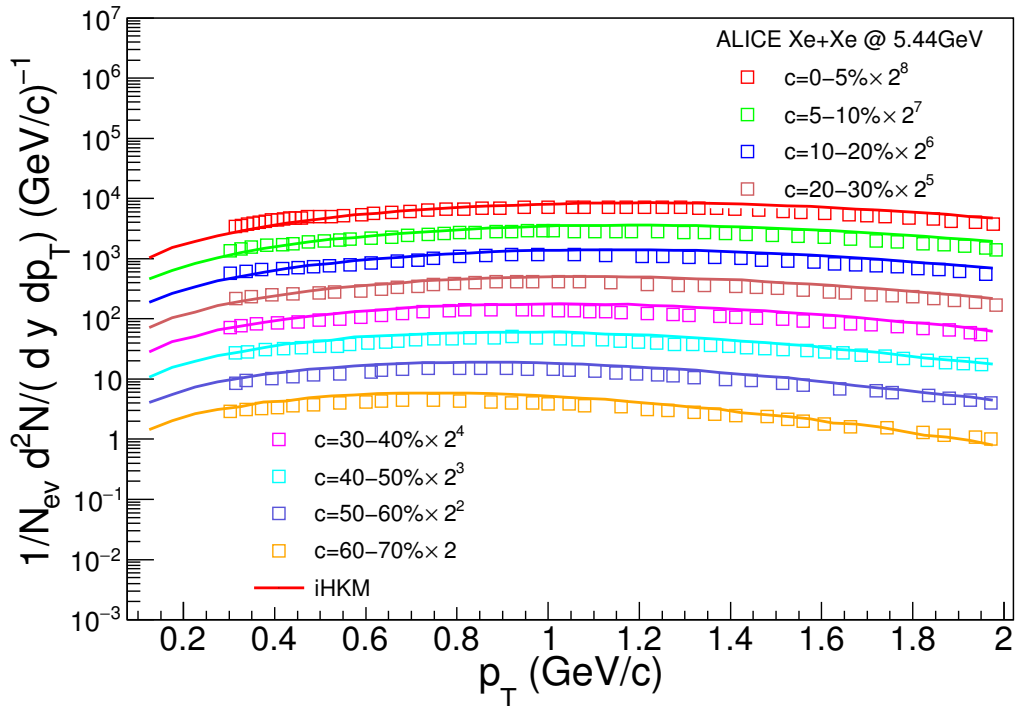


Figure 5. The same as in Figure 2 for protons, $|y| < 0.5$ (ALICE Collaboration points are taken from [21]).

In Figure 6, one can see the results of the calculation in iHKM for different particle number ratios in comparison with the experimental data from the ALICE Collaboration [22–24]. The points correspond to central collision events of Xe+Xe collisions at the LHC energy 5.44A TeV and previously analyzed within iHKM Pb+Pb collisions at the LHC energies 2.76A TeV and 5.02A TeV. The shown model points, corresponding to full iHKM calculation, which included inelastic processes at the afterburner stage,

were in good agreement with the data. The points for reduced regime without inelastic processes in most cases gave a worse or totally inadequate description of the experiment and thus are not shown. Most ratios of given particle yields for different collision types were close to each other, except for the ϕ/K ratio for the LHC energy 2.76A TeV. A possible reason for a lower value of the ϕ/K ratio in 2.76A TeV collisions could be the shorter and less intensive “afterburner” stage of matter evolution in this case, at which multiple particle scatterings took place, leading in particular to recombination of ϕ resonances from their decay products (kaons). This effect led to an increase of the observed ϕ yields, and so, if in the 5.02A TeV and 5.44A TeV cases, it is more pronounced, the corresponding ϕ/K ratios will be larger.

In general, summarizing the presented results, we concluded that iHKM successfully described the particle production in Xe+Xe collisions at the LHC energy $\sqrt{s_{NN}} = 5.44$ TeV, similarly to Pb+Pb collisions at the LHC and Au+Au collisions for RHIC cases, described in previous works. The final stage of the collision played an important role in the formation of bulk observables and supported the suggestion about the continuous character of the chemical and kinetic freeze-out.

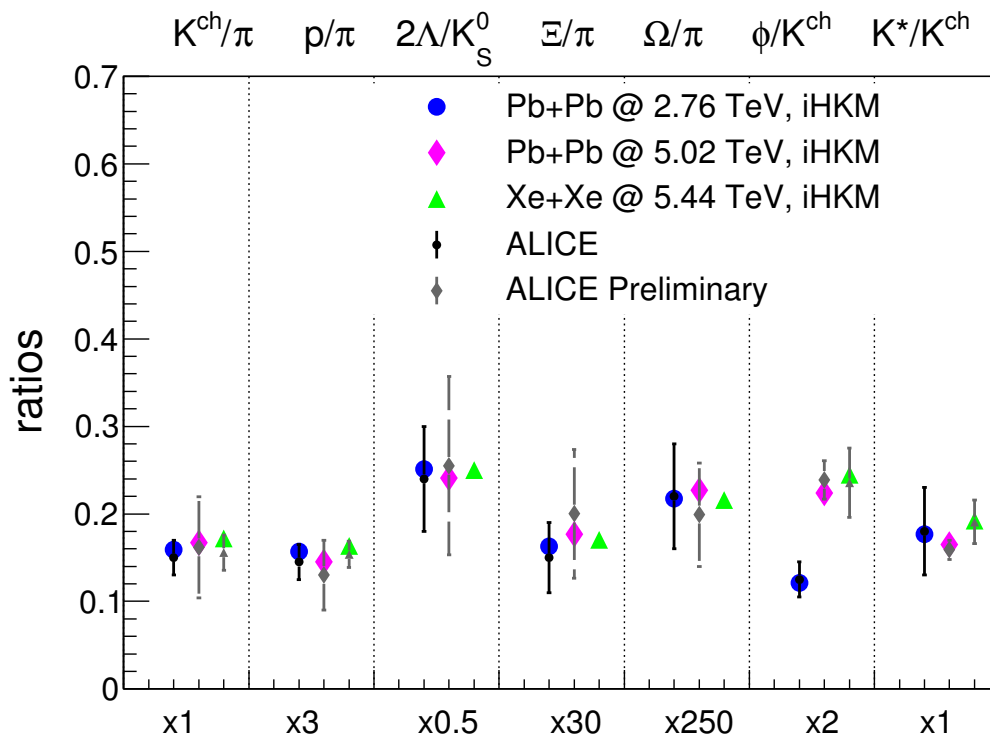


Figure 6. The iHKM results on various particle number ratios for central Pb+Pb collisions at the LHC energies $\sqrt{s_{NN}} = 2.76$ TeV and $\sqrt{s_{NN}} = 5.02$ TeV and Xe+Xe collisions at the LHC energy $\sqrt{s_{NN}} = 5.44$ TeV. The model points are compared to the experimental ones, where measured data are available [22–24].

Author Contributions: Conceptualization, Y.S.; data curation, M.A. and V.S.; funding acquisition, Y.S.; investigation, M.A. and V.S.; methodology, Y.S.; project administration, Y.S.; supervision, Y.S.; visualization, M.A. and V.S.; writing, original draft, V.S. All authors have read and agreed to the published version of the manuscript.

Funding: The research was carried out within the scope of the International Research Network “EUREA: European Ultra Relativistic Energies Agreement,” and the corresponding Agreement F20-2020 with the National Academy of Sciences (NAS) of Ukraine. The work was partially supported by the Tomsk State University Competitiveness Improvement Program.

Conflicts of Interest: The authors declare no conflict of interest. The funders had no role in the design of the study; in the collection, analyses, or interpretation of data; in the writing of the manuscript; nor in the decision to publish the results.

References

1. Adzhymambetov, M.D.; Shapoval, V.M.; Sinyukov, Y.M. Description of bulk observables in Au+Au collisions at top RHIC energy in the integrated hydrokinetic model. *Nucl. Phys. A* **2019**, *987*, 321–336. [[CrossRef](#)]
2. Naboka, V.Y.; Karpenko, I.A.; Sinyukov, Y.M. Thermalization, evolution, and observables at energies available at the CERN Large Hadron Collider in an integrated hydrokinetic model of A+A collisions. *Phys. Rev. C* **2016**, *93*, 024902. [[CrossRef](#)]
3. Shapoval, V.M.; Sinyukov, Y.M. Bulk observables in Pb+Pb collisions at $\sqrt{s_{NN}} = 5.02$ TeV at the CERN Large Hadron Collider within the integrated hydrokinetic model. *Phys. Rev. C* **2019**, *100*, 044905. [[CrossRef](#)]
4. Naboka, V.Y.; Akkelin, S.V.; Karpenko, I.A.; Sinyukov, Y.M. Initialization of hydrodynamics in relativistic heavy ion collisions with an energy-momentum transport model. *Phys. Rev. C* **2015**, *91*, 014906. [[CrossRef](#)]
5. Shapoval, V.M.; Braun-Munzinger, P.; Sinyukov, Y.M. $K^*(892)$ and $\phi(1020)$ production and their decay into the hadronic medium at the Large Hadron Collider. *Nucl. Phys. A* **2017**, *968*, 391–402. [[CrossRef](#)]
6. Sinyukov, Y.M.; Shapoval, V.M.; Naboka, V.Y. On m_T dependence of femtoscopy scales for meson and baryon pairs. *Nucl. Phys. A* **2016**, *946*, 227–239. [[CrossRef](#)]
7. Broniowski, W.; Rybczynski, M.; Bozek, P. GLISSANDO: GLauber Initial-State Simulation AND mOre. *Comput. Phys. Commun.* **2009**, *180*, 69–83. [[CrossRef](#)]
8. Acharya, S.; Acosta, F.T.; Adamova, D.; Adolfsson, J.; Aggarwal, M.M.; Aglieri Rinella, G.; Agnello, M.; Agrawal, N.; Ahammed, Z.; Ahn, S.U.; et al. Transverse momentum spectra and nuclear modification factors of charged particles in Xe-Xe collisions at $\sqrt{s_{NN}} = 5.44$ TeV. *Phys. Lett. B* **2019**, *788*, 166–179. [[CrossRef](#)]
9. Huovinen, P.; Petersen, H. Particlization in hybrid models. *Eur. Phys. J. A* **2012**, *48*, 171. [[CrossRef](#)]
10. Pratt, S. Accounting for backflow in hydrodynamic-Boltzmann interfaces. *Phys. Rev. C* **2014**, *89*, 024910. [[CrossRef](#)]
11. Molnar, D.; Wolff, Z. Self-consistent conversion of a viscous fluid to particles. *Phys. Rev. C* **2017**, *95*, 024903. [[CrossRef](#)]
12. Molnar, D. Identified particles from viscous hydrodynamics. *J. Phys. G* **2011**, *38*, 124173. [[CrossRef](#)]
13. Bass, S.A.; Belkacem, M.; Bleicher, M.; Brandstetter, M.; Bravina, L.; Ernst, C.; Gerland, L.; Hofmann, M.; Hofmann, S.; Konopka, J.; et al. Microscopic Models for Ultrarelativistic Heavy Ion Collisions. *Prog. Part. Nucl. Phys.* **1998**, *41*, 225–370. [[CrossRef](#)]
14. Bleicher, M.; Zabrodin, E.; Spieles, C.; Bass, S.A.; Ernst, C.; Soff, S.; Bravina, L.; Belkacem, M.; Weber, H.; Stocker, H.; et al. Relativistic Hadron-Hadron Collisions in the Ultra-Relativistic Quantum Molecular Dynamics Model. *J. Phys. G: Nucl. Part. Phys.* **1999**, *25*, 1859–1896. [[CrossRef](#)]
15. Giacalone, G.; Noronha-Hostler, J.; Luzum, M.; Ollitrault, J.-Y. Hydrodynamic predictions for 5.44 TeV Xe+Xe collisions. *Phys. Rev. C* **2018**, *97*, 034904. [[CrossRef](#)]
16. Giacalone, G.; Noronha-Hostler, J.; Luzum, M.; Ollitrault, J.-Y. Confronting hydrodynamic predictions with Xe-Xe data. *Nucl. Phys. A* **2019**, *982*, 371–374. [[CrossRef](#)]
17. Zhao, W.; Xu, H.J.; Song, H. Collective flow in 2.76 and 5.02 A TeV Pb + Pb collisions. *Eur. Phys. J. C* **2017**, *77*, 645. [[CrossRef](#)]
18. Bhalerao, R.S.; Jaiswal, A.; Pal, S. Collective flow in event-by-event partonic transport plus hydrodynamics hybrid approach. *Phys. Rev. C* **2015**, *92*, 014903. [[CrossRef](#)]
19. McDonald, S.; Shen, C.; Fillion-Gourdeau, F.; Jeon, S.; Gale, C. Hydrodynamic predictions for Pb+Pb collisions at 5.02 TeV. *Phys. Rev. C* **2017**, *95*, 064913. [[CrossRef](#)]
20. Bazavov, A.; Bhattacharya, T.; DeTar, C.; Ding, H.-T.; Gottlieb, S.; Gupta, R.; Hegde, P.; Heller, U.M.; Karsch, F.; Laermann, E.; et al. The equation of state in (2+1)-flavor QCD. *Phys. Rev. D* **2014**, *90*, 094503. [[CrossRef](#)]
21. Ragoni, S.; for the ALICE Collaboration. Production of pions, kaons and protons in Xe–Xe collisions at $\sqrt{s_{NN}} = 5.44$ TeV. *arXiv* **2018**, arXiv:1809.01086.
22. Floris, M. Hadron yields and the phase diagram of strongly interacting matter. *Nucl. Phys. A* **2014**, *931*, 103–112. [[CrossRef](#)]

23. Bellini, F.; for the ALICE Collaboration. Testing the system size dependence of hydrodynamical expansion and thermal particle production with π , K , p , and ϕ in Xe–Xe and Pb–Pb collisions with ALICE. *Nucl. Phys. A* **2019**, *982*, 427–430. [[CrossRef](#)]
24. Albuquerque, D.S.D.; for the ALICE Collaboration. Hadronic resonances, strange and multi-strange particle production in Xe–Xe and Pb–Pb collisions with ALICE at the LHC. *Nucl. Phys. A* **2019**, *982*, 823–826. [[CrossRef](#)]



© 2020 by the authors. Licensee MDPI, Basel, Switzerland. This article is an open access article distributed under the terms and conditions of the Creative Commons Attribution (CC BY) license (<http://creativecommons.org/licenses/by/4.0/>).